Optical spectroscopy and band gap analysis of hybrid improper ferroelectric $Ca_3Ti_2O_7$

Judy G. Cherian,[1] Turan Birol,[2] Nathan C. Harms,[1] Bin Gao,[2,3] Sang-Wook Cheong,[2,3] David Vanderbilt,[2] and Janice L. Musfeldt[1,4,a)]

[1)] *Department of Chemistry, University of Tennessee, Knoxville, Tennessee, 37996, USA*
[2)] *Department of Physics and Astronomy, Rutgers, The State University of New Jersey, Piscataway, New Jersey 08854, USA*
[3)] *Rutgers Center for Emergent Materials, Rutgers, The State University of New Jersey, Piscataway, New Jersey 08854, USA*
[4)] *Department of Physics, University of Tennessee, Knoxville, Tennessee, 37996, USA*

(Dated: 5 March 2016)

We bring together optical absorption spectroscopy, photoconductivity, and first principles calculations to reveal the electronic structure of the room temperature ferroelectric $Ca_3Ti_2O_7$. The 3.94 eV direct gap in $Ca_3Ti_2O_7$ is charge transfer in nature and significantly higher than that in $CaTiO_3$ (3.4 eV), a finding that we attribute to dimensional confinement in the n=2 member of the Ruddlesden-Popper series. While Sr substitution introduces disorder and broadens the gap edge slightly, oxygen deficiency reduces the gap to 3.7 eV and gives rise to a broad tail that persists to much lower energies.

I. INTRODUCTION

Ferroelectricity is one of the most useful and widely examined properties of the ABO_3 perovskites. $BaTiO_3$ and $PbTiO_3$ are flagship examples due to their spontaneous and switchable electric polarization.[1,2] The discovery of polarization in perovskite superlattices due to coupling of two rotational modes[3] motivated theoretical investigation that extended this idea to naturally occurring bulk materials that belong to the layered perovskite Ruddlesden-Popper ($A_{n+1}B_nX_{3n+1}$) series.[4,5] These studies identified two candidates as potential hybrid improper ferroelectrics: $Ca_3Ti_2O_7$ and $Ca_3Mn_2O_7$.[4,5] They are dubbed "improper" because ferroelectric polarization is not the primary order parameter, and the phrase "hybrid improper" indicates that the simultaneous onset of more than one primary order parameters (which are, in this case, oxygen octahedral rotations) is responsible for the emergence of the ferroelectric polarization.[6] While $Ca_3Ti_2O_7$ was already known to exist in a polar space group prior to these predictions,[4,7] the recent experimental discovery that it is indeed a *switchable* room temperature ferroelectric[8] is widely regarded as a materials design coup. This system sports a coercive field of 120 kV/cm and a net remanent electric polarization of 8 $\mu C/cm^2$ - values that compare well with proper ferroelectrics.[8] For instance, $BaTiO_3$ and $BiFeO_3$ films have coercive fields of 200 kV/cm and 140 kV/cm, respectively.[9,10] Interestingly, $CaTiO_3$ does not have a ferroelectric phase because the transition is suppressed by octahedral rotations.[11–13]

Unlike its close cousins (the prototypical titanate ferroelectric $BaTiO_3$ or strained Ruddlesden-Popper member $Sr_{n+1}Ti_nO_{3n+1}$ in which the polarization is driven by the displacement of the Ti cation),[15,16] the ferroelectric distortion in $Ca_3Ti_2O_7$ mostly involves displacement of the A-site Ca cations (Fig. 1).[8,17] The combined oxygen octahedral rotation/tilting modes that constitute the distortion result in layered dipoles that only partially cancel, yielding a net polarization due to the non-cancelling electric dipoles.[8] Charged domain walls (both ferroelectric and ferroelastic) are also present in this material.[8] The other physical properties are, at this time, unexplored.

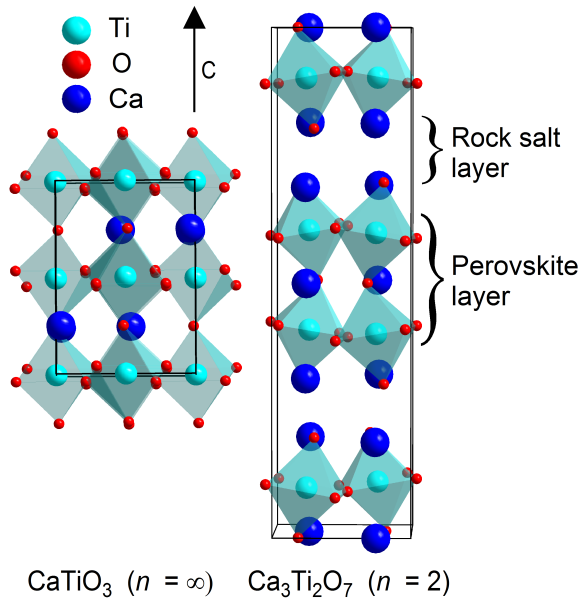

FIG. 1. (a) Crystal structure of $CaTiO_3$ illustrating the well-known three dimensionally-connected octahedra of the n=∞ material[14] and (b) the structure of $Ca_3Ti_2O_7$ which sports double layer slabs of perovskite units separated by CaO layers (n=2).[7] The properties of the $A_{n+1}B_nX_{3n+1}$ homologous series are mainly determined by the number of rock salt (charge storage) layers.

a)Electronic mail: musfeldt@utk.edu

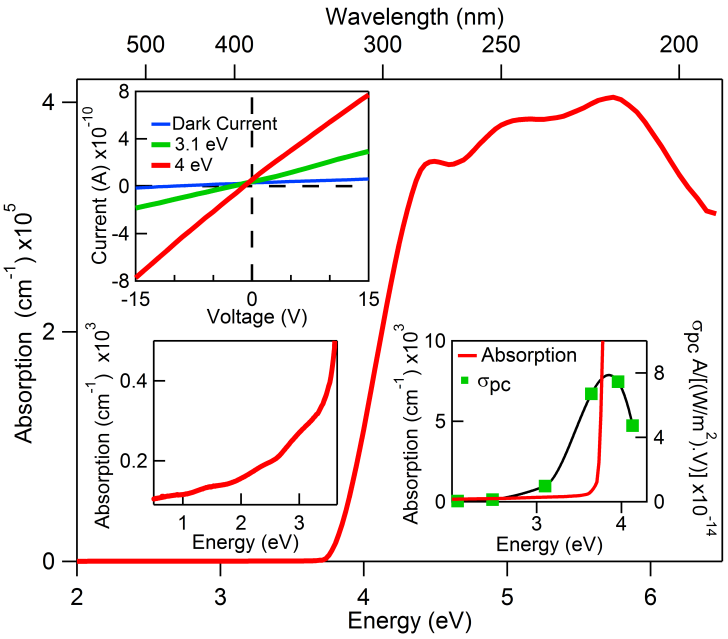

FIG. 2. Optical absorption spectrum of $Ca_3Ti_2O_7$ at 300 K. As discussed in the text, the band gap derives from charge transfer type excitations and is 3.94 eV. The lower left-hand inset shows a close-up view of the data below 3.5 eV. The upper inset displays typical I - V curves taken in the dark and under illumination at 3.1 and 4 eV. The lower right-hand inset compares the photoconductance taken at various photon energies with the absorption coefficient. The black curve is a guide to the eye.

Clearly, the opportunity to investigate the first new bulk room-temperature ferroelectric oxide in 50 years is a very exciting prospect. At the same time, the combination of octahedral rotations and ferroelectricity in perovskites is unusual[13] and merits additional investigation.

In this Letter, we report the optical properties of ferroelectric $Ca_3Ti_2O_7$ and compare our findings with complementary first principles calculations. We find a direct band gap of 3.94 eV, significantly larger than that of $CaTiO_3$ (3.4 eV). This is due to confinement effects in the n=2 member of the Ruddlesden-Popper series. Photoconductivity in $Ca_3Ti_2O_7$ tracks the absorption, with the largest response occurring just above the gap. We also explore the effects of A-site substitution and oxygen deficiency. Sr-substitution introduces disorder (which broadens the band edge slightly), whereas oxygen deficiency reduces the gap to 3.7 eV and gives rise to a broad tail that persists to much lower energies. These characteristics, combined with a natural ability to separate charge, suggest that $Ca_3Ti_2O_7$ and its derivatives may find applications in ultraviolet light harvesting and photo-catalysis.[18–20]

II. METHODS

High-quality single crystals of $Ca_3Ti_2O_7$, $Ca_{2.5}Sr_{0.5}Ti_2O_7$, and $Ca_3Ti_2O_{7-\delta}$ were grown using the optical floating zone method as described in Ref. 8. We employed a series of spectrometers and a combination of transmittance and reflectance techniques (on thinner and thicker samples, respectively) to extract the absorption coefficients. Photoconductivity experiments were carried out on crystals with sputtered Pt contacts using a setup that includes a Xenon source, a source measurement unit, a series of narrow bandpass filters, and tungsten contact tips. The response was normalized for power intensity and area. All experiments were carried out at room temperature.

First-principles calculations at the level of density functional theory (DFT) and generalized gradient approximation (GGA) were performed using the PBEsol exchange-correlation functional[21] and the projector augmented wave method[22,23] as implemented in VASP.[24,25] For the value of band gap, we report the energy difference between the highest occupied and lowest unoccupied Kohn-Sham states, which serves as a guide to understand the trends of the physical band gaps but does not directly correspond to a physically measurable quantity.

III. RESULTS AND DISCUSSION

A. Optical properties and electronic structure of $Ca_3Ti_2O_7$

Figure 2 displays the optical properties of $Ca_3Ti_2O_7$ at room temperature. The absorption is low and flat until nearly 4 eV, beyond which there is a sharp increase that defines the band gap and higher energy series of electronic excitations. Comparison with other perovskites like $CaTiO_3$ suggests that these features should be assigned as O $2p \rightarrow$ Ti $3d$ charge transfer excitations.[26,27] Traditionally, the magnitude and nature of the gap is determined from the spectroscopic response as:

$$\alpha(E) = \frac{A}{E}(E - E_{g,dir})^{0.5} + \frac{B}{E}(E - E_{g,ind} \mp E_{ph})^2, \quad (1)$$

where $\alpha(E)$ is the absorption coefficient, $E_{g,dir}$ is the direct gap energy, $E_{g,ind}$ is the indirect gap energy, E_{ph} is the mediating phonon energy, and A and B are constants.

Therefore, plots of $(\alpha \cdot E)^2$ vs energy and $(\alpha \cdot E)^{1/2}$ vs energy can reveal direct or indirect character via linear extrapolation to the energy axis.[28,29] As discussed in detail below, we find that $Ca_3Ti_2O_7$ has a direct gap of 3.94 eV. There is no evidence for indirect character. It is worth noting that, even though this type of analysis was developed for single parabolic band materials like traditional semiconductors,[29,30] it has been extended to include more complicated materials with non-parabolic bands such as oxides.[31–34]

In Figure 3, we report the densities of states of $CaTiO_3$ and $Ca_3Ti_2O_7$ determined from DFT. The d-orbitals of the Ti ions in $Ca_3Ti_2O_7$ are almost completely unoccupied and form the bottom of the conduction band, whereas the fully occupied oxygen p bands form the top of the valence band, which is also the case in bulk perovskite $CaTiO_3$. In both compounds, there is considerable hybridization between the oxygen and titanium states, and there is only a negligible amount of Ca density of states around the Fermi level. Even though the parent perovskite and Ruddlesden-Popper structures result in different symmetry environments for the ions, we find that the basic features of the band structure are similar, which is not surprising given their band insulating behaviours.

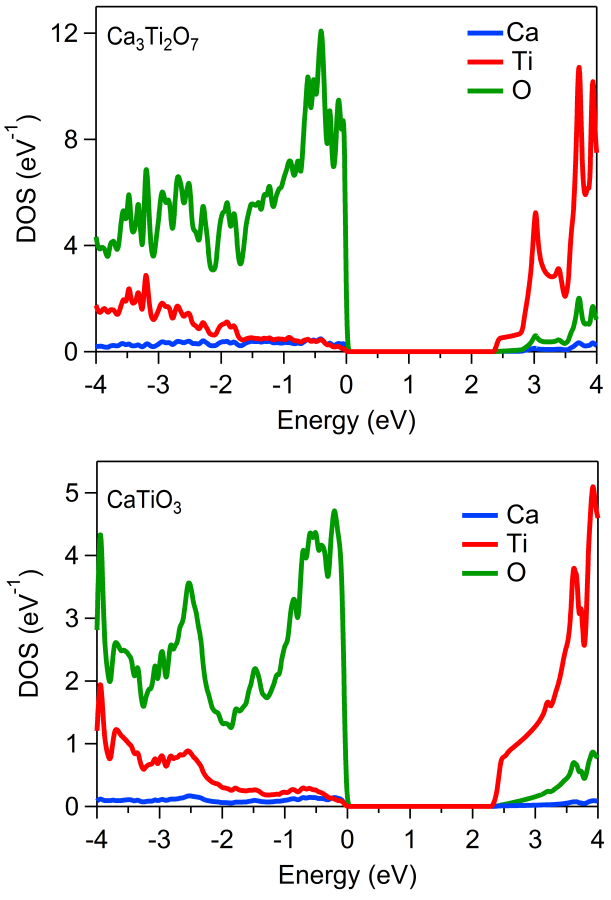

FIG. 3. Densities of states for $Ca_3Ti_2O_7$ and $CaTiO_3$ for the experimentally reported crystal structures from first principles.[35,36] The DOS are reported per formula unit and are projected onto the different atomic species.

We note that, according to our calculations, the band gap of $Ca_3Ti_2O_7$ (2.38 eV) is slightly larger than that of $CaTiO_3$ (2.30 eV). While DFT at the level of local density approximation (LDA) (or GGA) is usually considered sufficient to capture the trends of gaps in band insulators with different crystal structures, it has been reported in Ref. 37 that the trend of the gap between the bulk perovskite $SrTiO_3$ and the Ruddlesden-Popper compounds $Sr_{n+1}Ti_nO_{3n+1}$ is not correctly reproduced by DFT. However, DFT correctly captures the trends of the band gaps between different members of the $Sr_{n+1}Ti_nO_{3n+1}$ Ruddlesden-Popper series. Since the Ti d-states are unoccupied, this is probably not an error associated with the absence of strong on-site correlation effects in DFT. Rather, it might be necessary to calculate the full optical response, including the effect of electron-hole interactions, to capture the correct trend of the band gaps,[37] which is beyond the scope of this work. At this stage, we merely note that if the $CaTiO_3$ related compounds behave similarly to their closely related $SrTiO_3$ cousins, we would anticipate $Ca_3Ti_2O_7$ to have an even larger gap than $CaTiO_3$ in the light of our calculations and previous work on $Sr_{n+1}Ti_nO_{3n+1}$.[37] This point is verified by our measurements as discussed below.

B. Photoconductivity of $Ca_3Ti_2O_7$

We also sought to evaluate the ability of $Ca_3Ti_2O_7$ to create photocarriers. The upper inset of Fig. 2 displays typical I-V curves with light on and off, and the lower right-hand inset shows the photoconductance at different illumination energies. Clearly, there is a strong correlation between the absorption coefficient and photoconductivity. Moreover, it is well known that photocurrent increases near or above the band gap.[38] This is because photoconductivity is related to absorption as:[39]

$$\sigma_{PC} \propto \eta\alpha(E)\tau, \tag{2}$$

where σ_{PC} is the photoconductance of the sample, η is the quantum efficiency (defined as ratio of excited carriers created to the number of incident photons), $\alpha(E)$ is the absorption, and τ is the carrier life time. From Eq. 2, it is clear that as absorption rises, the photoconductance should also increase. This trend is evident in the similarity between σ_{PC} and $\alpha(E)$ in $Ca_3Ti_2O_7$. Our analysis shows that current loss takes place predominantly via space-charge-limited conduction, similar to the mechanism in other perovskites.[40,41] We estimate a charge mobility on the order 10^{-4} cm^2/V·s.

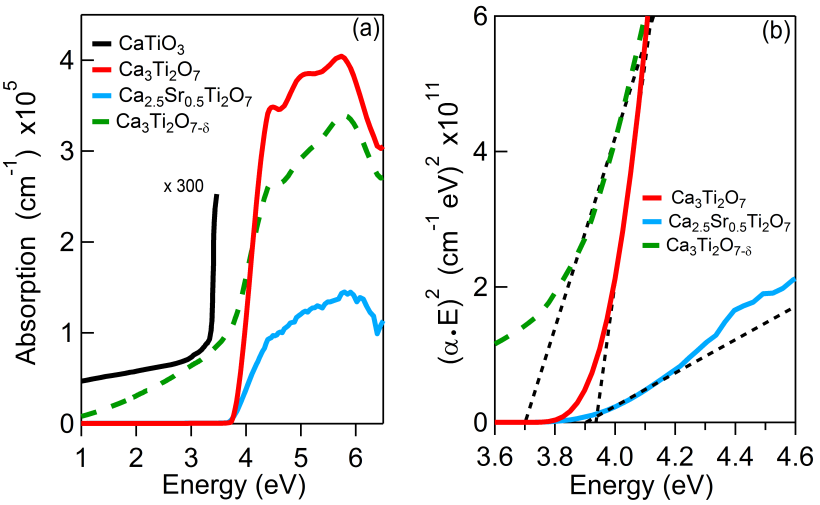

FIG. 4. (a) Absorption spectrum of $Ca_3Ti_2O_7$ along with that of the Sr-substituted counterpart and the oxygen deficient analog. The response of $CaTiO_3$ from Ref. 42 is included for comparison. (b) Direct band gap analysis of these materials. The optical gap of $Ca_3Ti_2O_7$ is 3.94 eV, whereas that of the Sr-substituted and oxygen deficient systems are 3.9 and 3.7 eV, respectively.

C. Comparison of related materials

Figure 4 summarizes the optical absorption and direct gap analysis of $Ca_3Ti_2O_7$ and compares the findings with those of $CaTiO_3$, $Ca_{2.5}Sr_{0.5}Ti_2O_7$, and $Ca_3Ti_2O_{7-\delta}$. This series provides a platform with which we can assess the structure-property relationships connected with dimensionality and confinement, *A*-site substitution-related disorder, and oxygen deficiency.

1. $Ca_3Ti_2O_7$ vs. $CaTiO_3$ and dimensionality effects

Figure 4 displays the optical response and band gap analysis of $Ca_3Ti_2O_7$ compared with that of $CaTiO_3$.[42] We immediately notice that the onset of charge transfer excitations in $CaTiO_3$ occurs at a significantly lower energy compared to that in the n=2 member of the Ruddlesden-Popper series. Accordingly, the direct gap of $CaTiO_3$ has been reported to be 3.4 eV.[42] This comparison (3.94 vs. 3.4 eV) directly reveals the effect of reduced dimensionality on the electronic properties. A similar variation has been reported in $SrTiO_3$ (and its associated layered series).[37] This trend is typical in layered perovskites including the Ruddlesden-Popper series[43,44] due to the fact that the octahedra, which are three-dimensionally connected in the n=∞ parent compound, become systematically disconnected with decreasing n. At the same time, the orbitals defining the band edge become increasingly confined, which narrows the valence band and increases the gap.[37] Our calculations (Fig. 3) uncover the same trend.

2. Sr substitution on the *A* site

Chemical substitution is a powerful technique for tuning the properties of layered perovskites.[45] This approach is motivated by the fact that stability lies in the tolerance factor, which is characterized by the relative size of the cations involved. In our work, we replaced Ca with Sr to yield $Ca_{2.5}Sr_{0.5}Ti_2O_7$. Figure 4(a) displays the optical response of $Ca_{2.5}Sr_{0.5}Ti_2O_7$; the corresponding direct gap analysis is shown in panel (b). Ca-related states are not involved in the excitations that define the leading edge of the band gap. That said, the relative size difference between Sr and Ca ions is significant, and it is the Ca ions in the perovskite layer (and not the ones in the rock salt layer) that get replaced by Sr.[7] Consequently, the octahedral rotation and tilt angle are reduced to stabilize the structure.[7,8] Since octahedral rotations in perovskites often control the electronic structure and properties,[46–48] we anticipated the band gap to be modulated due to Sr substitution. In fact, our analysis instead reveals a band gap of 3.9 eV, which is just slightly lower than the 3.94 eV gap for $Ca_3Ti_2O_7$. This is in line with our DFT calculations that find that when the degree of octahedral rotations are decreased in $Ca_3Ti_2O_7$, the band gap is reduced by a minute amount [Supplementary information]. We also find that the band edge is broadened slightly compared to pristine $Ca_3Ti_2O_7$. We conclude that chemical disorder in $Ca_{2.5}Sr_{0.5}Ti_2O_7$ decreases the band gap only slightly whereas it reduces the net remnant polarization by 50% compared to the parent compound.[8]

3. The role of oxygen deficiency

Trends in the electronic structure that develop due to oxygen deficiencies in the Ruddlesden-Popper series are particularly interesting because the valence band is primarily comprised of O 2*p* orbitals [Fig. 3]. As a result, oxygen vacancies introduce carriers, modify the band width, and at the same time distort the local lattice environment.[18,49,50] Figure 4 (a, b) displays the optical absorption spectrum and corresponding direct gap analysis of $Ca_3Ti_2O_{7-\delta}$, respectively. The band gap of

$Ca_3Ti_2O_{7-\delta}$ is 3.7 eV, significantly lower than that of pristine $Ca_3Ti_2O_7$. This is because oxygen vacancies introduce hole carriers and they might also geometrically modify the TiO_6 octahedral rotations, which result in a broader valence band. The broad tail that persists to much lower energies for the oxygen-deficient sample in Fig. 4 (a) is similar to the response of oxygen deficient $CaTiO_3$ and $SrTiO_3$.[51,52] Clearly, control of the oxygen content is a promising strategy for band gap tuning in $Ca_3Ti_2O_7$; the technique has been used successfully in many other materials as well.[53] At the same time, gating experiments, particularly those carried out with ionic liquids, should be carefully controlled to prevent oxygen migration.

IV. CONCLUSION

To summarize, we combined optical spectroscopy, photoconductivity, and first principles calculations to unveil the electronic properties of $Ca_3Ti_2O_7$, the first bulk room-temperature ferroelectric oxide discovered in the last 50 years. Analysis of the linear absorption spectrum reveals a direct gap at 3.94 eV, significantly larger than that in $CaTiO_3$ (3.4 eV) due to confinement effects in the n=2 member of the Ruddlesden-Popper series. The band gap in $Ca_3Ti_2O_7$ is defined by O $p \rightarrow$ Ti d charge transfer excitations. A-site chemical substitution with Sr broadens the gap ever so slightly, an effect that we attribute to the influence of octahedral tilting. On the other hand, oxygen vacancies reduce the band gap to 3.7 eV and introduce a significant low energy tail. Both effects are due to the addition of charge carriers and the associated valence band broadening. An obvious extension of this work is to investigate B site substitution[18] in $Ca_3Ti_2O_7$ and $Ca_3Ti_2O_{7-\delta}$. This may lead to new and interesting families of magnetoelectric multiferroics.

V. ACKNOWLEDGEMENTS

Research at Tennessee is supported by the U.S. Department of Energy, Office of Basic Energy Sciences, Materials Science Division under Award DE-FG02-01ER45885 (JLM). Work performed at Rutgers is supported by the National Science Foundation under Award DMREF-1233349 (SWC and DV).

[1] R. E. Cohen, Nature **358**, 136 (1992).
[2] A. von Hippel, Rev. Mod. Phys. **22**, 221 (1950).
[3] E. Bousquet, M. Dawber, N. Stucki, C. Lichtensteiger, P. Hermet, S. Gariglio, J.-M. Triscone, and P. Ghosez, Nature **452**, 732 (2008).
[4] N. A. Benedek and C. J. Fennie, Phys. Rev. Lett. **106** (2011).
[5] A. B. Harris, Phys. Rev. B **84** (2011).
[6] S.-W. Cheong and M. Mostovoy, Nat. Mater. **6**, 13 (2007).
[7] M. M. Elcombe, E. H. Kisi, K. D. Hawkins, T. J. White, P. Goodman, and S. Matheson, Acta Crystallogr., Sect. B: Struct. Sci **47**, 305 (1991).
[8] Y. S. Oh, X. Luo, F.-T. Huang, Y. Wang, and S.-W. Cheong, Nat. Mater. **14**, 407 (2015).
[9] J. Y. Jo, Y. S. Kim, T. W. Noh, J.-G. Yoon, and T. K. Song, Appl. Phys. Lett. **89**, 232909 (2006).
[10] J. Wang, J. B. Neaton, H. Zheng, V. Nagarajan, S. B. Ogale, B. Liu, D. Viehland, V. Vaithyanathan, D. G. Schlom, U. V. Waghmare, N. A. Spaldin, K. M. Rabe, M. Wuttig, and R. Ramesh, Science **299**, 1719 (2003).
[11] W. Zhong and D. Vanderbilt, Phys. Rev. Lett. **74**, 2587 (1995).
[12] V. V. Lemanov, A. V. Sotnikov, E. P. Smirnova, M. Weihnacht, and R. Kunze, Solid State Commun. **110**, 611 (1999).
[13] N. A. Benedek and C. J. Fennie, J. Phys. Chem. C **117**, 13339 (2013).
[14] A. Beran, E. Libowitzky, and T. Armbruster, Can. Mineral. **34**, 803 (1996).
[15] N. A. Benedek and T. Birol, J. Mater. Chem. C (2016), 10.1039/C5TC03856A.
[16] T. Birol, N. A. Benedek, and C. J. Fennie, Phys. Rev. Lett. **107**, 257602 (2011).
[17] N. A. Benedek, A. T. Mulder, and C. J. Fennie, J. Solid State Chem. **195**, 11 (2012).
[18] W. L. Harrigan, S. E. Michaud, K. A. Lehuta, and K. R. Kittilstved, Chem. Mater. **28**, 430 (2016).
[19] Y. Sang, H. Liu, and A. Umar, ChemCatChem **7**, 559 (2015).
[20] H. Kato and A. Kudo, J. Phys. Chem. B **106**, 5029 (2002).
[21] J. P. Perdew, K. Burke, and M. Ernzerhof, Phys. Rev. Lett. **77**, 3865 (1996).
[22] P. E. Blöchl, Phys. Rev. B **50**, 17953 (1994).
[23] G. Kresse and D. Joubert, Phys. Rev. B **59**, 1758 (1999).
[24] G. Kresse and J. Furthmüller, Phys. Rev. B **54**, 11169 (1996).
[25] G. Kresse and J. Furthmüller, Comput. Mater. Sci. **6**, 15 (1996).
[26] K. Ueda, H. Yanagi, R. Noshiro, H. Hosono, and H. Kawazoe, J. Phys.: Condens. Matter **10**, 3669 (1998).
[27] A. H. Kahn and A. J. Leyendecker, Phys. Rev. **135**, A1321 (1964).
[28] J. Tauc, Mater. Res. Bull. **3**, 37 (1968).
[29] J. I. Pankove, *Optical processes in semiconductors* (Dover, New York, 1971).
[30] J. Tauc, R. Grigorovici, and A. Vancu, Phys. Status Solidi B **15**, 627 (1966).
[31] E. Rey, M. R. Kamal, R. B. Miles, and B. S. H. Royce, J. Mater. Sci. **13**, 812 (1978).
[32] B. D. Viezbicke, S. Patel, B. E. Davis, and D. P. Birnie, Phys. Status Solidi B **252**, 1700 (2015).
[33] Q. C. Sun, H. Sims, D. Mazumdar, J. X. Ma, B. S. Holinsworth, K. R. O'Neal, G. Kim, W. H. Butler, A. Gupta, and J. L. Musfeldt, Phys. Rev. B **86**, 205106 (2012).
[34] B. S. Holinsworth, D. Mazumdar, H. Sims, Q.-C. Sun, M. K. Yurtisigi, S. K. Sarker, A. Gupta, W. H. Butler, and J. L. Musfeldt, Appl. Phys. Lett. **103**, 082406 (2013).
[35] L. H. Oliveira, A. P. de Moura, T. M. Mazzo, M. A. Ramírez, L. S. Cavalcante, S. G. Antonio, W. Avansi, V. R. Mastelaro, E. Longo, and J. A. Varela, Mater. Chem. Phys. **136**, 130 (2012).
[36] K. Hawkins and T. J. White, Phil. Trans. R. Soc. A **336**, 541 (1991).
[37] C.-H. Lee, N. J. Podraza, Y. Zhu, R. F. Berger, S. Shen, M. Sestak, R. W. Collins, L. F. Kourkoutis, J. A. Mundy, H. Wang, Q. Mao, X. Xi, L. J. Brillson, J. B. Neaton, D. A. Muller, and D. G. Schlom, Appl. Phys. Lett. **102**, 122901 (2013).
[38] R. H. Bube, *Photoelectronic Properties of Semiconductors* (Cambridge University Press, 1992).
[39] M. Brinza, J. Willekens, M. Benkhedir, and G. Adriaenssens, in *Springer Handbook of Electronic and Photonic Materials*, edited by S. Kasap and P. Capper (Springer US, 2006) p. 137.
[40] G. W. Pabst, L. W. Martin, Y.-H. Chu, and R. Ramesh, Appl. Phys. Lett. **90**, 072902 (2007).
[41] F. D. Morrison, P. Zubko, D. J. Jung, J. F. Scott, P. Baxter, M. M. Saad, R. M. Bowman, and J. M. Gregg, Appl. Phys. Lett. **86**, 152903 (2005).
[42] A. Linz and K. Herrington, J. Chem. Phys. **28**, 824 (1958).
[43] C. Grote, B. Ehrlich, and R. F. Berger, Phys. Rev. B **90**, 205202 (2014).

[44]Z.-T. Zhu, J. L. Musfeldt, H.-J. Koo, M.-H. Whangbo, Z. S. Teweldemedhin, and M. Greenblatt, Chem. Mater. **14**, 2607 (2002).
[45]T. Wolfram and S. Ellialtioglu, *Electronic and Optical Properties of d-Band Perovskites* (Cambridge University Press, Cambridge, 2006).
[46]A. T. Mulder, N. A. Benedek, J. M. Rondinelli, and C. J. Fennie, Adv. Funct. Mater. **23**, 4810 (2013).
[47]M. J. Pitcher, P. Mandal, M. S. Dyer, J. Alaria, P. Borisov, H. Niu, J. B. Claridge, and M. J. Rosseinsky, Science **347**, 420 (2015).
[48]F. Li, C. Song, Y. Y. Wang, B. Cui, H. J. Mao, J. J. Peng, S. N. Li, G. Y. Wang, and F. Pan, Sci. Rep. **5**, 16187 (2015).
[49]H. Liu, F. Zeng, Y. Lin, G. Wang, and F. Pan, Appl. Phys. Lett. **102**, 181908 (2013).
[50]C. Mitra, C. Lin, J. Robertson, and A. A. Demkov, Phys. Rev. B **86**, 155105 (2012).
[51]J. Milanez, A. T. d. Figueiredo, S. d. Lazaro, V. M. Longo, R. Erlo, V. R. Mastelaro, R. W. A. Franco, E. Longo, and J. A. Varela, J. Appl. Phys. **106**, 043526 (2009).
[52]E. Orhan, F. M. Pontes, M. A. Santos, E. R. Leite, A. Beltrán, J. Andrés, T. M. Boschi, P. S. Pizani, J. A. Varela, C. A. Taft, and E. Longo, J. Phys. Chem. B **108**, 9221 (2004).
[53]S. R. Basu, L. W. Martin, Y. H. Chu, M. Gajek, R. Ramesh, R. C. Rai, X. Xu, and J. L. Musfeldt, Appl. Phys. Lett. **92**, 091905 (2008).